UC San Diego
UC San Diego Electronic Theses and Dissertations

Title

Regulation of the Circadian Clock Function in Arabidopsis thaliana by the Bacterial Pathogen Pseudomonas syringae

Permalink

Author

Turkalj, Elena

Publication Date

2019

Peer reviewed|Thesis/dissertation

UNIVERSITY OF CALIFORNIA SAN DIEGO

Regulation of the Circadian Clock Function in *Arabidopsis thaliana* by the Bacterial Pathogen

Pseudomonas syringae

A Thesis submitted in partial satisfaction of the
requirements for the degree Master of Science

in

Biology

By

Elena Martina Turkalj

Committee in charge:

      Professor Jose L. Pruneda-Paz, Chair
      Professor Mark Estelle
      Professor Martin F. Yanofsky

2019

The Thesis of Elena Martina Turkalj is approved, and it is acceptable in quality and form for publication on microfilm and electronically:

_____

_____

_____

Chair

University of California San Diego

2019

DEDICATION

I would like to dedicate my Thesis to my Baka Zlata, my Grandmother Lesley, and my Mother for their unwavering support during my graduate program. They have all taught me at a young age to appreciate school, but more importantly, to appreciate the sciences. They have set amazing examples of what women can achieve when given an opportunity to become educated.

EPIGRAPH

"Discovery consists of looking at the same thing as everyone else and thinking something different." - Albert Szent-Gyorgyi

TABLE OF CONTENTS

LIST OF FIGURES

LIST OF TABLES

ACKNOWLEDGEMENTS

ABSTRACT OF THE THESIS

Regulation of the Circadian Clock Function in *Arabidopsis thaliana* by the Bacterial Pathogen

Pseudomonas syringae

by

Elena Martina Turkalj

Master of Science in Biology

University of California San Diego 2019

Professor Jose L. Pruneda-Paz, Chair

An internal time keeping mechanism known as the circadian clock allows organisms to anticipate changes in the environment (Michael et al., 2003; Dodd, 2005). Environmental stressors have been shown to disrupt the circadian clock so it cannot accurately predict those changes. For example, a previous study revealed that a *Pseudomonas syringae* infection altered

the clock, leading to long period and dampened circadian rhythms (Li et al., 2018). These clock phenotypes were triggered by host and pathogen responses (Li et al., 2018). In this thesis, we explored the molecular mechanisms that regulate the observed clock phenotypes upon infection. We found that pathogen-triggered responses directly target clock components, which likely results in the observed clock phenotypes. Such results suggest that, at least in plants, the outcome of host-pathogen interactions relies on the control of the circadian clock function.

Introduction

It is evolutionarily advantageous for organisms to have an internal time-keeping system (Dodd, 2005). This mechanism, the circadian clock, allows plants to anticipate environmental changes and adjust their physiological responses accordingly (Michael et al., 2003). For example, young sunflowers track the sun's movement across the sky based on timing information from their circadian clock. If the sunflowers cannot predict that the sun will rise in the east at dawn and instead face west, they will receive reduced sunlight and therefore will not photosynthesize as efficiently. In fact, a study confirmed that east-facing sunflowers have more biomass and are more fit relative to their west-facing counterparts (Atamian et al., 2016).

The circadian clock is an endogenous biological clock that runs in an approximately 24-hour cycle and can persist in constant conditions (McClung, 2006).The gears of the clock consist of circadian proteins that regulate each other through interlocked feedback loops(McClung, 2006). In the model organism, *Arabidopsis Thaliana*, the core feedback loop consists of two morning-expressed MYB transcription factors, CIRCADIAN CLOCK ASSOCIATED 1 (CCA1) and LONG ELONGATED HYPOCOTYL (LHY) (Figure 1). In the evening, the transcription factor expressed is a pseudo response regulator known as TIMING OF CAB EXPRESSION1 (TOC1). CCA1 and LHY negatively regulate TOC1 expression at the beginning of the day (Alabadí et al., 2001). As the day progresses, CCA1 and LHY protein levels are downregulated which relieves the transcriptional repression of TOC1. TOC1 protein levels peak at the beginning of the evening and repress the transcription of CCA1 and LHY (Nakamichi et al., 2010). In the hours before dawn, TOC1 is ubiquitinated and degraded by the 26s proteasome which relieves the transcriptional repression of CCA1 and LHY (Más et al., 2003b). TOC1 ubiquitination is mediated by a SKIP-CULLIN-FBOX (SCF) complex that contains an F-box protein

ZEITELUPE (ZTL) which specifically binds to TOC1 (Gagne et al., 2002). ZTL regulation of TOC1 is a critical component of the plant's core clock mechanism (Más et al., 2003b).

Maintaining stable clock function is important for optimal plant fitness (Dodd, 2005).When the clock malfunctions (i.e. due to mutations in clock proteins), synchrony between the endogenous clock and the environment is disrupted. This leads to sub-optimal plant growth (Dodd, 2005). For example, CCA1, LHY, and TOC1 single mutants all lead to a short period phenotype of about 20 hours (Dodd, 2005).They also show abnormal growth (i.e. hypocotyl elongation) and abnormal developmental (i.e. flowering time) phenotypes compared to wild-type plants (Más et al., 2003; Strayer et al., 2000). Interestingly, when TOC1 mutants and wild-type *Arabidopsis* were subjected to a 20-hour day, the TOC1 mutants were found to be more fit than the wild-type in those conditions (Dodd, 2005).This result further illustrates that the resonance between the endogenous clock and the environmental rhythms are critical to achieve optimal plant performance. It is not fully understood why mutating CCA1, LHY, or TOC1 leads to a shorter period, but it is known that the *Arabidopsis* clock is highly sensitive to TOC1 abundance (Más et al., 2003). More specifically, high TOC1 levels lengthen the period while low levels shorten it (Más et al., 2003a). ZTL regulation of TOC1 levels is therefore essential to maintain the period of the plant clock. In fact, ZTL loss-of-function results in a long period phenotype which is attributed to TOC1 protein being more stable and therefore more abundant (Más et al., 2003a).

Mutated clock proteins have been shown to desynchronize the endogenous clock with the environment (Somers et al., 1998; Lu et al., 2009). In addition, environmental inputs like biotic stressors have also been shown to alter the clock function (Li et al., 2018; Zhang et al., 2013). To defend against these stressors, plants use defense mechanisms to respond to the pathogen

2

invasion (Nürnberger and Brunner, 2002). When a pathogen associated molecular pattern (PAMP) such as bacterial flagella binds to a specific plant receptor on the plasma membrane, a host response known as PAMP triggered immunity (PTI) is initiated (Nürnberger and Brunner, 2002). This response leads to a cascade of signaling proteins that ultimately activate defense genes (Boller and Felix, 2009; Pitzschke and Hirt, 2009). Some pathogens inhibit immune responses by injecting virulence proteins known as effectors. In the case of *Pseudomonas syringae pv tomato DC3000 (PstDC3000)*, it uses a type three secretion system (T3SS) which requires a pilus to inject pathogenic effectors to subdue the host's PTI (Jones and Dangl, 2006). Not only have effectors been known to hijack immune responses, but they have also been found to promote their pathogenicity by altering plant metabolism and host degradation machinery (Djamei et al., 2011; Mathieu et al., 2014). A recent study found that *PstDC3000* infection led to a long period phenotype in non-infected tissues (Li et al., 2018). This was thought to be caused by Salicylic Acid (SA) and Reactive Oxygen Species (ROS) components of the PTI response. However, when plants were individually treated with SA and H202, the long period phenotype could not be recovered. This experiment suggests that it was not a PTI induced effect on the clock, but potentially a pathogenic response (Li et al., 2018).

Building on these findings, the main goal of our project was to investigate if *PstDC3000* may be altering the clock function. Our work identified a specific *PstDC3000* effector, AvrPto, that interacts with the TOC1 protein. Such interaction alters TOC1 protein stability providing a mechanism for the regulation of clock period upon the infection of *PstDC3000*.
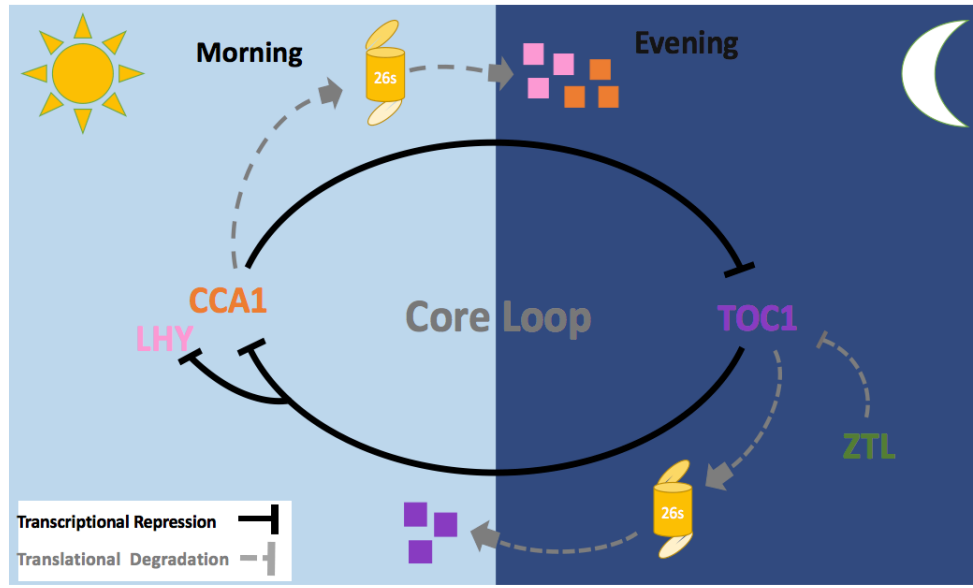
Figure 1. Diagram depicting the feedback mechanism of morning and evening clock proteins in *Arabidopsis thaliana*. The morning transcription factors CIRCADIAN CLOCK ASSOCIATED 1 (CCA1) and LATE ELONGATED HYPOCOTYL (LHY) repress transcription of the evening transcriptional regulator TIMING OF CAB EXPRESSION 1 (TOC1). CCA1 and LHY are degraded as the day progresses, which relieves the transcriptional repression on *TOC1*. Increased TOC1 levels transcriptionally repress *CCA1* and *LHY* in the evening. Towards the late evening/early morning, ZEITELUPE (ZTL) targets TOC1 for degradation via the 26s proteasome, which allows *CCA1* and *LHY* upregulation and reinitiates the loop.
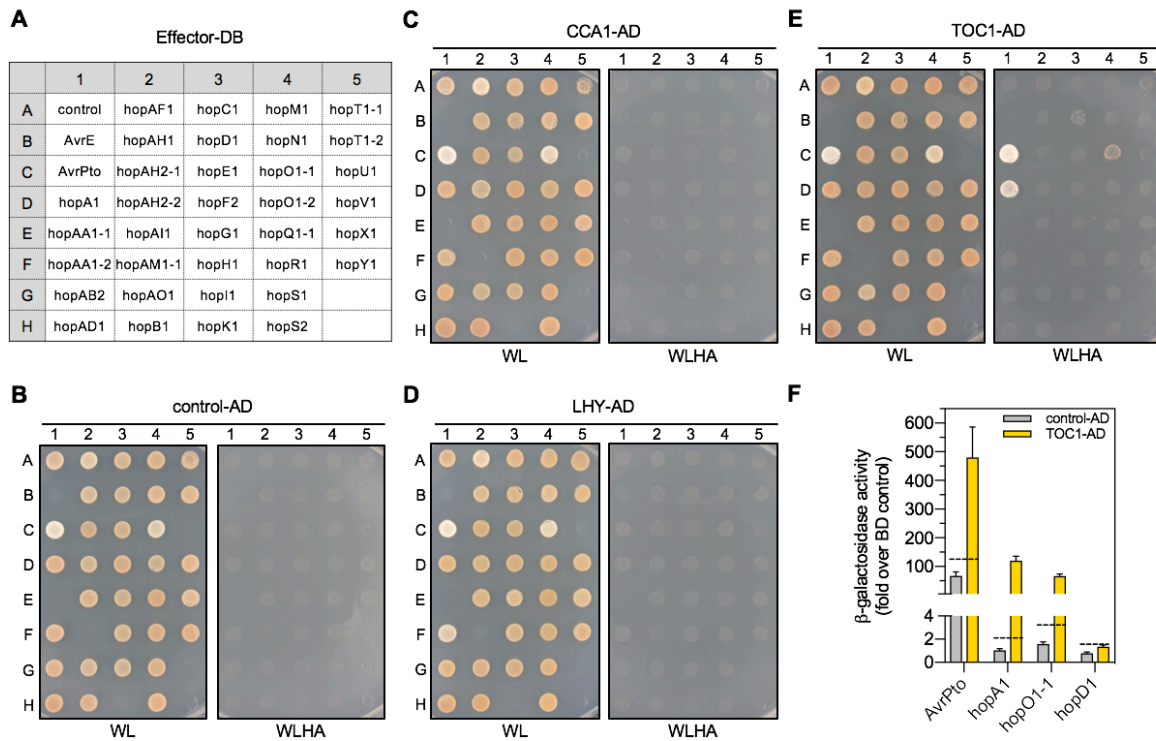
Results

P.syringae **effectors bind to core clock protein, TOC1**.

Previous research has shown that *P. syringae pv. tomato DC3000* infection in *Arabidopsis thaliana* results in a period lengthening of clock oscillations in non-infected tissues (Li et al., 2018). During *P.syringae* infection, effectors are injected into the host which inhibit components of immune response pathways (Jones and Dangl, 2006). Combined experimental evidence indicates that the observed clock phenotype is induced by *Pst* DC3000 virulence factors and not by the activation of host immune responses (Li et al., 2018). Because the period lengthening could not be attributed to defense response, we hypothesized that it must be cause by the virulence factors. To explore this hypothesis, we investigated whether Pst DC3000 effectors could interact with the core clock proteins TOC1, CCA1, and LHY. These clock proteins were selected because they are particularly important in determining the clock period. To analyze protein-protein interactions in a medium scale format we used a yeast two-hybrid (Y2H) system. We began by creating a complete collection of *P.syringae* effector proteins fused to the gal4 activation domain. Next, we generated TOC1, CCA1, and LHY fusions to the Gal4 DNA binding domain. Cells containing each pairwise combination of AD and DBD constructs were then tested for their ability to produce the auxotrophic selection markers ADE2 and HIS3. This experiment revealed that four effectors, AvrPto, hopA1, hopO1-1, hopD1 interacted with the TOC1 protein (Figure 2A-D). To further confirm these results we additionally tested if positive interactions were also revealed using the enzymatic selection marker lacZ (Figure 2F). Our results were consistent for TOC1 interaction with AvrPto, hopA1 and hopO1-1, but not hopD1. Further, quantification of the β-galactosidase activity allowed us to rank AvrPto as the top TOC1-interacting effector. Altogether, these experiments allowed us to generate a full collection

of PstDC3000 effector clones suitable for Y2H experiments and uncovered for the first time that

the PstDC3000 effectors AvrPto, hopA1, hopO1-1 can interact with core clock proteins. Because

AvrPto had the highest B-galactosidase activity, we decide to focus our work on AvrPto to better

understand how effectors may affect TOC1 clock functions.

Figure 2. TOC1 interacts with AvrPto, hopA1 and hopO1-1 in yeast.
A) Array of bait effector constructs fused to the Gal4 DNA binding domain (DB) used in B, C, D and E. **B, C, D and E)** yeast two-hybrid experiment results using the constructs indicated in A) and prey control (B), CCA1 (C), LHY (D) and TOC1 (E) constructs fused to the Gal4 activation domain (AD). Cells grown in WL medium were replica-plated onto WLHA selection medium to identify protein-protein interactions. F) Quantification of β-galactosidase activity for the interactions found in B, C, D and E.

Effector AvrPto binds to TOC1 *in vivo*

Since we found that AvrPto interacts with TOC1 in yeast cells, we hypothesized that they would interact *in planta*. To test this hypothesis, we conducted a Bimolecular Fluorescence Complementation Assay (BiFC) in *Nicotiana benthamiana* leaves. In this assay, two proteins fused to complementary non-fluorescent halves of the Yellow fluorescent protein (YFP) can reconstitute the fluorescence emission of YFP only if the proteins interact with each other. To test AvrPto-TOC1 interaction using BiFC, we generated constructs carrying the plant constitutive Cauliflour Mosaic Virus 35S promoter carrying the TOC1 or AvrPto coding sequence fused to the N-terminal or C-terminal region of YFP. Agrobacterium carrying these constructs were co-infiltrated into *N. benthamiana* leaves for transient expression of both fusion proteins. Fluorescence was monitored with a confocal microscope. A strong fluorescence signal was only detected in leaves that co-expressed TOC1 and AvrPto (Figure 3D), but not in the controls (Figure 3A,B,C). The confirmation of TOC1-AvrPto interaction in *planta* supports our previous Y2H findings. This finding proves for the first time that a pathogen can directly target a clock protein and supports our idea that *P.syringae* may be manipulating the clock function.
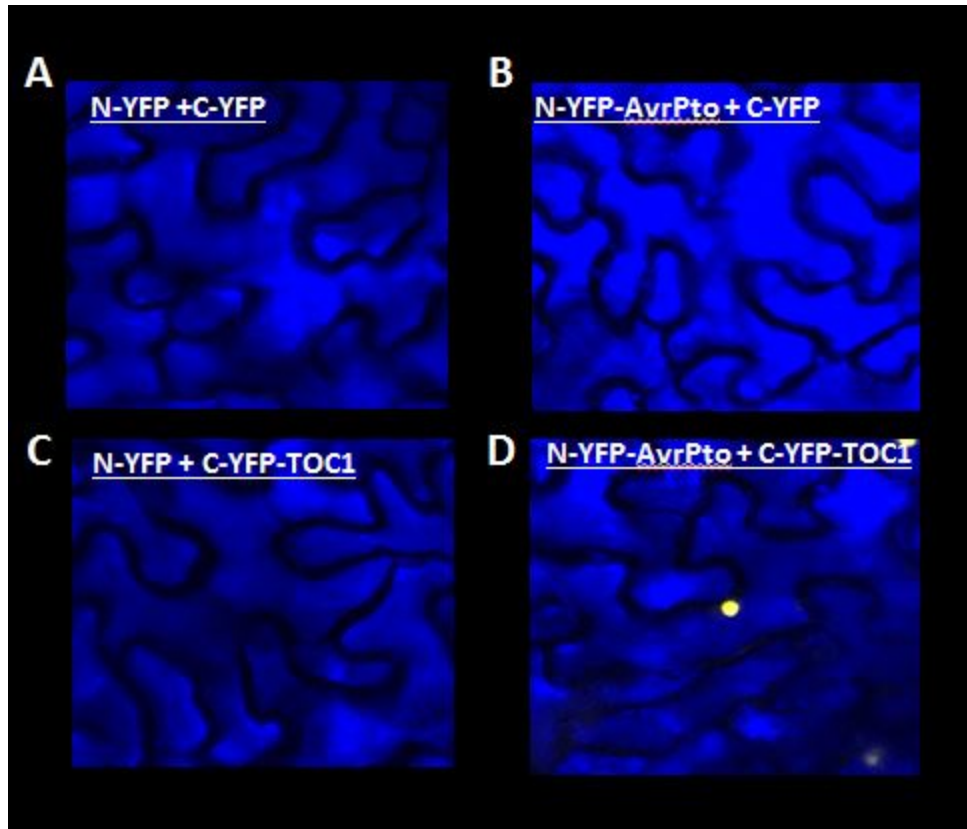
Figure 3. TOC1 interacts with AvrPto in *Planta*. Bimolecular Fluorescence complementation assay conducted in *Nicotiana benthamiana*. 48 hours after infection images were taken. YFP and pseudo colored brightfield images were merged. **A)** YFP N-terminus and C-terminus co-expressed **B)** YFP N-terminus fused to AvrPto and YFP C-terminus. **C)** YFP N-terminus and YFP C-terminus fused to TOC1. **D)** YFP N-terminus fused to AvrPto and YFP C-terminus fused to TOC1.

AvrPto induction leads to a period lengthening in Arabidopsis

Previous work has revealed that *P.syringae* infection led to a longer period phenotype in core clock promoters fused to luciferase (Li et al., 2018). It is also known that TOC1 protein abundance determines the period of clock controlled rhythms (Más et al., 2003). Since we found that AvrPto interacts with TOC1 in *planta*, we hypothesized that AvrPto induction may similarly lead to period changes. To test this idea, we decided to generate a transgenic line (XVE::AvrPto-14.3) that would conditionally overexpress AvrPto when plants are exposed to Estradiol. In addition, these plants also carry a clock reporter (*CCA1::LUC+*) which allowed us to monitor the circadian rhythms. Analysis of the luciferase reporter activity after estradiol treatment in wild-type (control) and XVE::AvrPto plants indicated that AvrPto induction produced ~2 hour period lengthening in the whole plant relative to the control (Figure 4A,4B). This result indicates that the AvrPto effector alone is sufficient to cause clock period lengthening. Furthermore, we expect that this relationship extends to AvrPto introduced during *P.syringae* infection.
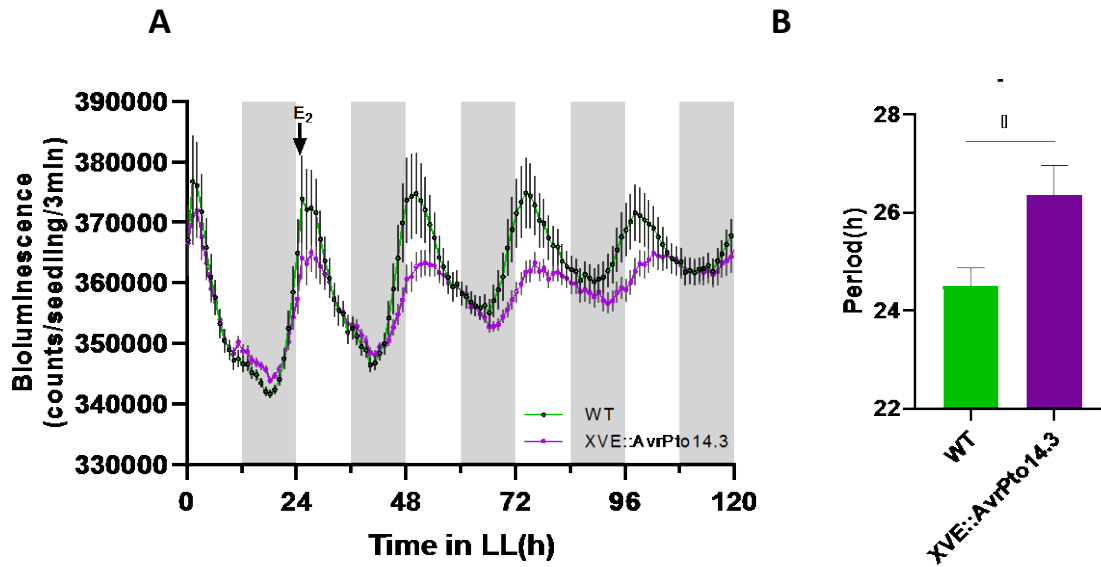
Figure 4. AvrPto induction causes longer period in *Arabidopsis*. Arabidopsis seedlings were grown for 8 days in LD conditions(12hr light/12 hr dark) at 22°C. Estradiol treatment (50uM) were sprayed at the 25th hour in LL conditions at 22°C. Results indicate +/- SEM, n=16, and are representative of three individual experiments. **A)** Luciferase activity was monitored for 6 days. **B)** Average period was analyzed from hours 37-108.

AvrPto and ZTL do not interact

AvrPto expression has been shown to cause a long period phenotype of ~26 hours. TOC1 levels have also been linked to period changes (Más et al., 2003). Lower levels lead to a shorter period and higher level leads to a longer period phenotype (Más et al., 2003). A regulator of TOC1, ZTL has been found to have a long period when mutated which was attributed to TOC1 abundance (Más et al., 2003). Since AvrPto interacts with TOC1 and was found to lengthen the period, we hypothesized that AvrPto may have a role in modulating TOC1 stability. One way AvrPto could reduce TOC1 degradation would be to form a trimeric complex with ZTL and TOC1. If AvrPto binds to both then it is possible that it could inhibit the function of ZTL. To determine if AvrPto interacts with ZTL, we conducted a Y2H. We monitored the growth of yeast on -WLHA selection plates. We found no yeast growth when AvrPto and ZTL were co-expressed indicating that AvrPto and ZTL do not interact. This result reveals that AvrPto is not forming a complex with ZTL and TOC1, but is interacting solely with TOC1.
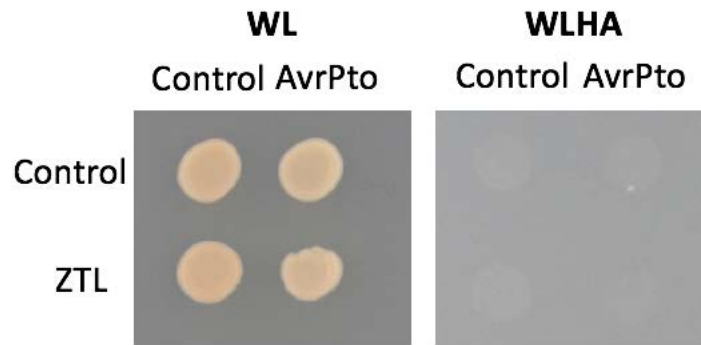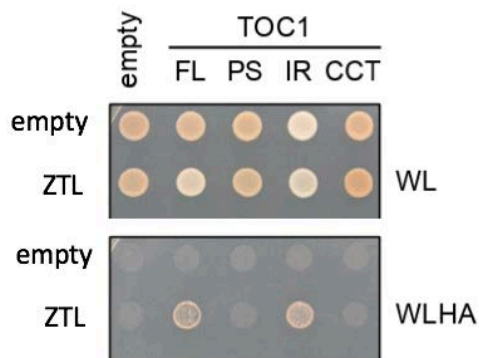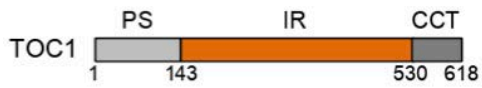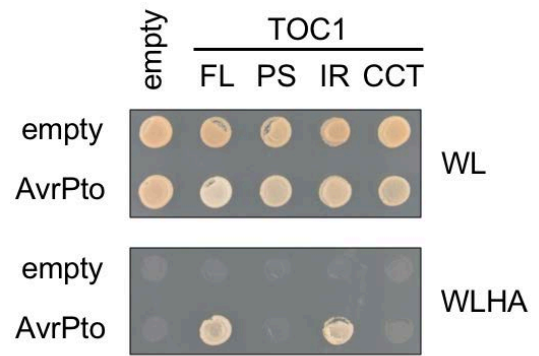
Figure 5. AvrPto and ZTL do not interact in yeast.
ZTL constructs were fused to the Gal4 DNA binding domain. AvrPto was fused to the Gal4 activation domain. Cells grown in WL medium were replica-plated onto WLHA selection medium to identify protein-protein interactions.

AvrPto and ZTL binds to TOC1 domain, IR

Based on our findings, AvrPto does not interact with ZTL and therefore does not form a complex with TOC1 and ZTL. We hypothesized that AvrPto may be interacting with a similar domain to ZTL which could stabilize TOC1. To better understand the molecular mechanism behind AvrPto and ZTL binding to TOC1, we conducted a Y2H screen. We separated TOC1 into three domains PS (1-143 aa), IR (143-530 aa), and CCT (530-618 aa). The pseudo receiver (PS) domain is a conserved region between pseudo response regulators (PRRS)(Nakamichi et al., 2010) . It is similar to the two component system in response regulators, but PRRS lack Aspartate residues (Makino et al., 2000). These Asp residues are normally found to be phosphorylated by a sensor kinase (Makino et al., 2000). In previous studies, the PS domain was found to repress CCA1 and LHY transcription (Nakamichi et al., 2010). The intermediate (IR) domain is a region unique to TOC1 and not associated with other PRRS (Nakamichi et al., 2010). This region has been previously shown to bind to another evening protein, EARLY FLOWERING 3 (ELF3), but the mechanism of this interaction is not completely understood yet(Huang et al., 2016). The Constans, CO-like, TOC1 (CCT) domain is a conserved region between those three proteins (Strayer et al., 2000) . It is also a conserved sequence between PRRS. CCT has been found to regulate flowering time (Putterill, 2001; Strayer et al., 2000; Wenkel et al., 2006). In our Y2H screen, as expected, we found that both AvrPto and ZTL bind to the full length TOC1. Interestingly, they also bind to the IR domain (Figure 6A,6B). Firstly, these results indicate that both AvrPto and ZTL bind to TOC1 in a unique way that is not conserved between PRRS. Secondly, since they both bind to the same domain, it is possible that AvrPto may be blocking ZTL binding to TOC1.

Figure 6. AvrPto and ZTL bind to TOC1-IR in yeast.
 A,B) TOC1 constructs were fused to the Gal4 DNA binding domain. ZTL and AvrPto were fused to the Gal4 activation domain. Cells grown in WL medium were replica-plated onto WLHA selection medium to identify protein-protein interactions.

AvrPto disrupts the binding of ZTL to TOC1

Based on our previous results, AvrPto was not found to bind to ZTL, but was found to bind to the same IR region on TOC1. We hypothesized that there was competitive binding occurring. We conducted a yeast three hybrid(Y3H) between AvrPto, TOC1, and ZTL. In this system, we monitored the binding of TOC1 and ZTL with the presence or absence of AvrPto. As expected, TOC1 and ZTL interacted without the presence of AvrPto (Figure 7). Interestingly, when all three proteins were co-expressed, the interaction between ZTL and TOC1 were disrupted. These results indicates that AvrPto blocks ZTL binding to TOC1 which suggests there is in fact competitive binding.
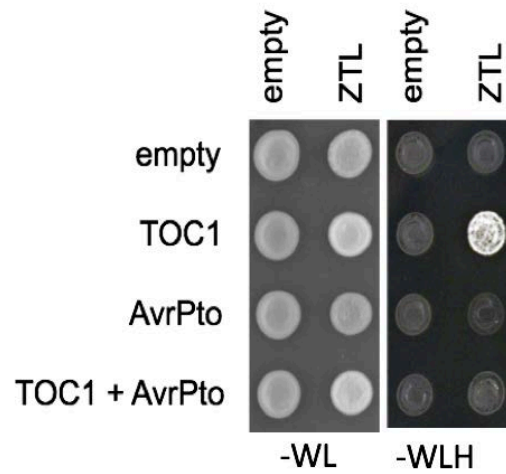
Figure 7. AvrPto disrupts binding of ZTL with TOC1 in yeast.
TOC1 construct was fused to the Gal4 DNA binding domain. ZTL was fused to the Gal4 activation domain. AvrPto was fused to a methionine inducible promoter. Cells grown in WL medium were replica-plated onto WLH selection medium without methionine to identify protein-protein interactions.

Discussion

The circadian clock is an important mechanism for synchronizing physiological rhythms with the environment. When the clock is not able to adjust the rhythmic outputs to match the environmental cycles, this leads to a reduction in plant fitness (Dodd, 2005). Environmental stressors like pathogen infections have been shown to change the clock function in plants (Li et al., 2018). Until now the molecular mechanism behind the clock changes had not been uncovered. Our work revealed that three *P.syringae* effectors (AvrPto, hopA1, hopO1-1) target an evening clock protein,TOC1, in yeast. AvrPto was shown to interact with TOC1 in planta and cause a period lengthening of ~2 hours when AvrPto was induced in transgenic *Arabidopsis* lines. This period lengthening is consistent with our previous work which shows that an infection with *P.syringae* also led to a period lengthening (Li et al., 2018). In that paper, the period change was found to be 30 minutes in non-infected tissues which slightly differs from our findings of ~2 hours in the whole plant. One possible explanation for this discrepancy is that there may be a higher concentration of AvrPto in the inducible lines than in the infection which leads to a longer period. Another possible reason is that during an infection, the presence of the pathogen can trigger plant defense responses that may counteract the period changes induced by bacterial effectors. In fact, Li et al. noticed a phase advance which was linked to SA and H202 defense responses from the host. This phase advance may explain the modest period lengthening of only 30 minutes found post infection. The longer period observed in the infection context indicated that pathogens may have evolved mechanisms to regulate the clock function. Our work fully supports this notion and was the first to find a direct link between pathogen effector proteins, such as AvrPto, and core clock components, which may play a role in clock regulation after infection.

Period changes due to pathogenic infections have been found in mammals as well. A study found that an infection with *Trypanosoma brucei* (*T .brucei*) led to a period shortening in mice (Rijo-Ferreira et al., 2018).This short period was not a result of inflammation or defense responses, but most likely due to the pathogen itself. Similarly, in another mammal study, a viral infection with influenza A virus (IAV) in mice resulted in a period lengthening (Sundar et al., 2015). These studies support the idea that pathogen regulation of the clock period is a conserved response between mammals and plants. In the case of *T. brucei,* the period change led to a shortening as opposed to a lengthening as observed in our work and in IAV infection. This suggests that not all pathogens interact with the clock in the same way. Regardless of the specific period change, alterations in the clock pace will desynchronize the clock with the environment (Dodd, 2005). If the clock becomes out of sync with the environment, it may not be able to adjust its defense responses in time with the infection (Zhang et al., 2013). Thus, clock mis regulation may be a novel mechanism used by pathogens to evade host immune responses.

To better understand how AvrPto may have a role in the infection context, following experiments should test if a *P. syringae* mutant, only expressing AvrPto, also triggers clock period lengthening. We hypothesize that AvrPto in the infection context will have similar effects to inducing AvrPto in *Arabidopsis*. To further confirm that the period lengthening is attributed to the pathogen effectors, a *P.syringae* mutant that cannot inject effectors could also be used in experiments that monitor the clock function. After the role of effectors in the infection context is established, the effector-clock molecular mechanism should be further explored. To better understand if AvrPto stabilizes TOC1, an inducible AvrPto line should be used to monitor the amount of TOC1. If TOC1 is stabilized, we hypothesize that there will be an abundance of TOC1 even during the time of day when TOC1 is expected to be targeted by ZTL for degradation. After

establishing a connection between AvrPto and TOC1 stability, a TOC1 knock out in an AvrPto inducible line should be conducted to monitor for period changes. If AvrPto binding to TOC1 is in fact leading to period changes as presented in this paper, there should be no difference in the period. A deeper understanding of the TOC1-AvrPto mechanism will allow researchers to design transgenic plants that will be immune to pathogenic effects on the clock function.

Materials and Methods

Construction of pENTR/D vectors

The pENTR/D-TOC1 (Pruneda-Paz, 2009), pENTR/D-ZTL (ref) and pENTR/D-MCS (Bonaldi et al, unpublished) vectors were previously described.

To build pENTR/D-effectors, pENTR/D-TOC1(ns), pENTR/D-TOC1(PS), pENTR/D-TOC1(IR), pENTR/D-TOC1(CCT) and pENTR/D-ZTL(LOV) vectors, the coding regions for *Pseudomonas syringae* pv. *tomato* DC3000 *(Pst* DC3000*)* effector proteins, TOC1 without a stop codon (ns) or deletion construct (PS: pseudoresponse regulator domain, IR: intermediate region and CCT: CONSTANS-CO-like-TOC1 domain), and ZTL-LOV domain were PCR amplified from *Pst* DC3000 genomic DNA, pENTR/D-TOC1 and pENTR/D-ZTL, respectively (primers indicated in table S1). PCR products were cloned into pENTR/D-TOPO (Life technologies). To build pENTR/D-SII(ns), the coding region for the strepII epitope without a stop codon Fw primer 5'-CACCATGTGGAGCCACCCTCAATTTGAAAAGTGA-3' and Rvs 5'-CTTTTCAAATTGAGGGTGGCTCCACATGGTG-3' were primer annealed and cloned into pENTR/D-TOPO (Life technologies).

To build pENTR/D-AvrPto(ns), the coding region for the AvrPto effector without a stop codon was PCR amplified from pENTR/D-AvrPto (primers indicated in table S1) and cloned into pENTR/D-TOPO (Life technologies).

To build pENTR/D-AvrPto(Y89D), the full plasmid carrying a T to G transversion in nucleotide 265 of the AvrPto protein coding sequence was PCR amplified from pENTR/D-AvrPto using the partially overlapping primers 5'-ATGCAGCATAGG<u>G</u>ACATGACGGGAGCGTCAGG-3' and 5'-

T<u>C</u>CCTATGCTGCATGTCCGCCATATCCAGTGTTC-3'. The resulting PCR product was circularized using NEBuilder HiFi DNA Assembly (New England Biolabs).

Plant Materials

Arabidopsis thaliana (Arabidopsis) seedlings used in this work were from the Columbia ecotype (Col-0). *CCA::LUC+* (Pruneda-Paz, 2009) and *TOC1::YFP-TOC1 (CAB2::LUC)* (Más et al., 2003) lines were previously described.

To generate β-estradiol inducible *AvrPto* and *AvrPto(Y89D)* overexpression lines (*XVE-AvrPto* and *XVE- AvrPto(Y89D)*), pENTR/D-AvrPto and pENTR/D-AvrPto(Y89D) vectors wer used to transfer coding sequences into the pMDC7 binary vector (Curtis, 2003) using LR Clonase II (Life Technologies). pMDC7-AvrPto and pMDC7-AvrPto(Y89D) vectors, and the empty control vector pMDC7-MCS (Bonaldi et al., unpublished), were transformed into Arabidopsis *CCA1::LUC+* plants via Agrobacterium mediated transformation as described before (Zhang et al., 2006)

To generate *toc1^{CR-2}*, a deletion of 247 bp between nucleotide 19 (exon 1) and 266 (intron 1) of the *TOC1* coding region was generated using CRISPR-CAS9 genome editing. Briefly, two guide RNA (gRNA$_1$: 5'- GATTTGAACGGTGAGTGTAA-3' and gRNA$_2$: 5'-GTCTGGCTTTTTGAGTCAGTA-3') encoding genes (*U6-26$_{pro}$::gRNA$_1$-U6-26$_{ter}$* and *U6-29$_{pro}$::gRNA$_2$-U6-26$_{ter}$*) were PCR amplified in tandem and cloned at the *Bam*HI site of the binary vector p3J1 (Ripoll-Samper and Pruneda-Paz, unpublished) and transformed into Arabidopsis Col-0 plants via Agrobacterium mediated transformation as described before (Zhang et al., 2006). T1 plants were PCR genotyped using the following primers: 5'-GCGACTTTGTAGGGACACTG-3' and 5'-TCGATATCAGGTCCCTCTGC-3'. Transgene-

free plants were selected at the T2 generation and hereditability of the deletion was confirmed in each of 4 generations backcrossed to Col-0.

Bioluminescence imaging upon single leaf *P. syringae* infections

Arabidopsis *CCA::LUC+* seeds were surface sterilized and stratified in the dark at 4°C for two days. Stratified seeds were grown in autoclaved soil (Sunshine professional mix, Sungro) under 12h light (~100 μmol.m^{-2}.s^{-1}) / 12h dark cycles (LD) for 14 days at 22°C. At the beginning of day 14 (one day before the imaging period started) plants were sprayed with 5mM of D-lucifernin potassium salt (in 0.01% triton X-100 solution) and watered (3ml per plant) with 5mM D-lucifernin potassium salt (in water solution). At the beginning of day 15, plants were transferred to constant light (60 μmol.m^{-2}.s^{-1}, 22°C) (LL) for bioluminescence imaging. Bioluminescence was quantified every 1h using a Pixis 1024 CCD camera (Princeton Instruments) for 7 days.

Single leaf infections were performed at the beginning of the second day in LL (ZT25). For that, *Pst* DC3000 wild-type or hrpA mutant (*Pst* DC3000-hrpA) (Wei et al., 2000) were grown in liquid cultures (King's B medium: 2% Proteose peptone No.3, 1% Glycerol, 8.6mM K_2HPO_4 and 6mM $MgSO_4$) in the dark at 28°C (shaking at 175rpm) until OD600 between 0.6 and 0.7 was reached (several dilutions were started to assure that a suitable culture was available at the time of treatment). Bacteria were harvested by centrifugation at 3220 x *g* for 2min, resuspended in sterile water (LabChem), and harvested by centrifugation at 3220 x *g* for 3min. The bacterial pellet was resuspended in water (LabChem) adjusting OD600 to 0.2 (~1x10^8 cfu), and Silwet L77 (Lehle seeds) was added to a final concentration of 0.025%. About half of a single leaf was dipped into this cell suspension or a mock solution (0.025% Silwet L77) for

1min. After treatment, excess inoculum was blot-dried from the leaf surface using a sterile filter paper strip.

Bioluminescence imaging upon conditional *AvrPto* overexpression

Seeds of Arabidopsis *CCA::LUC+* carring the XVE-MCS (control), XVE-AvrPto or XVE-AvrPto(Y89D) β-estradiol inducible overexpression construct were surface sterilized and stratified in the dark at 4°C for two days. Stratified seeds were grown at 22 $^{\circ}$C in 12 hours light (100 µmol.m^{-2}.s^{-1}) / 12 hours dark cycles on 1.5 % agar Murashige-Skoog (MS) medium supplemented with 3 % sucrose. At the beginning of day 9 (one day before the imaging period started) plants were sprayed with 5mM of D-luciferin potassium salt (in 0.01% triton X-100 solution). At the beginning of day 10, plants were transferred to constant light (60 µmol.m^{-2}.s^{-1}, 22°C) (LL) for bioluminescence imaging. Bioluminescence was quantified every 1h using a Pixis 1024 CCD camera (Princeton Instruments) for 7 days. β-estradiol treatments were performed at the beginning of the second day in LL (ZT25) by spraying seedlings with β-estradiol (25 µM or 50 µM) or mock solutions (in 0.01 % Triton X-100).

Bioluminescence data analysis

Bioluminescence images were processed using the MetaMorph image analysis software (Molecular Devices) to determine bioluminescence counts (for plate and soil grown plants) and number of bioluminescent pixels (for soil grown plants) per plant or for a specific tissue section. To estimate plant size across an entire time course experiment, a third-order polynomial curve was regressed from the experimental pixel count data using GraphPad Prism version 6 (GraphPad Software, www.graphpad.com) (curve fitting was used to minimize pixel count bias

due to plant movement and unequal signal bleeding due to rhythmic bioluminescence levels).

Bioluminescence counts (for plate grown seedlings) and plant size normalized bioluminescence values (for soil grown plants or tissue sections) for each experiment were analyzed by Fast Fourier Transform-Non Linear Least Squares (FFT-NLLS) (Plautz et al., 1997) using the interface provided by the Biological Rhythms Analysis Software System (BRASS) (Julio et al., 2006). Amplitude changes within each experiment were calculated as the ratio between the amplitude value obtained for each individual (both for mock and treated plants) and the mean amplitude obtained for mock treated plants (amplitude change = individual amplitude / mean amplitude mock) ($\log_{10}$ transformed ratios were used for statistical analysis). Normalized phase values were calculated as [24*(t-24)/p], where p is the period of the corresponding individual plant calculated by BRASS and t is the fitted acrophase time closest to the second subjective morning (ZT24) extrapolated using BRASS. Normalized phase mean values were calculated using an R circular statistics package (Agostinelli and Lund, 2011). Phase shifts were calculated by subtracting the normalized phase of each individual from the mean normalized phase of mock treated plants (phase shift = mean phase mock – individual phase) (phase advance or delay were indicated by positive or negative values respectively). Normalized phase versus relative amplitude error circular plots were generated using an R "polar.plot" function (Marshall et al., 2016).

Biomass measurement

Tissue collection was performed at the end of single leaf *P. syringae* infection experiments (single plant aerial tissues). Fresh weight was determined immediately after tissue collection and dry weight was determined after 12 days of incubation at 37ºC.

mRNA transcript quantification

Seeds of Arabidopsis *CCA::LUC+* carring the XVE-MCS (control), XVE-AvrPto or XVE-AvrPto(Y89D) β-estradiol inducible overexpression construct were surface sterilized and stratified in the dark at 4°C for two days. Stratified seeds were grown at 22 $^{\circ}$C in 12 hours light (100 µmol.m^{-2}.s^{-1}) / 12 hours dark cycles on 1.5 % agar Murashige-Skoog (MS) medium supplemented with 3 % sucrose. At the beginning of day 9 plants were sprayed with β-estradiol (25 µM or 50 µM) or mock solutions (in 0.01 % Triton X-100). At the beginning of day 10, pools of ~20 seedlings per genotype/treatment were collected and were snap frozen in liquid nitrogen. Total RNA from these samples was isolated using the RNeasy plant mini kit (Qiagen) and on-column DNAse (Roche) treatment. For cDNA synthesis, 1µg of total RNA was reverse-transcribed using the iScript cDNA synthesis kit (Bio-Rad). Transcript levels in each sample were determined by real time quantitative PCR (qPCR) (Bio-Rad CFX96 Real-time PCR detection system) using the Maxima Sybr green qPCR mix (Life Technologies), and the following PCR conditions: 95°C for 10 minutes, 40 cycles of 95°C for 10 seconds, 60°C for 20 seconds, and 72°C for 25 seconds. qPCR primer sequences were: 5'GGTGACGAAGATAACGTAACGT3' and 5'GCTTTGAGGTGCTTGGTTACT3' for *AvrPto*, and 5'-TAACGTGGCCAAAATGATGC3' and 5'-GTTCTCCACAACCGATTGGT-3' for *PP2A*. Gene expression levels were normalized to the reference gene for *PP2A* using the comparative Ct method (Schmittgen and Livak, 2008) and then to the mean expression of mock samples within each biological replicate. Statistical analyses were performed using GraphPad Prism version 8.

Bimolecular fluorescence complementation (BiFC) assay

The gene silencing inhibitor pCB-P19HA (*35S::P19-HA*) plasmid was previously described (Chapman et al., 2004).

To generate **pSITE-cEYFP-N1-TOC1, pSITE-EYFP-N1-SII, pSITE-nEYFP-N1-AvrPto and pSITE-nEYFP-N1-SII** vectors, AvrPto, TOC1 and StrepII (control) protein coding sequences were transferred from pENTR/D-AvrPto(ns), pENTR/D-TOC1(ns) and pENTR/D-SII(ns) into the **pSITE-nEYFP-N1** and/or **pSITE-cEYFP-N1** binary vectors (Godio and Martín, 2009) using LR Clonase II (Life Technologies).

To prepare plants, *Nicotiana benthamiana* seeds were surface sterilized and stratified in the dark at 4°C for two days. Stratified seeds were grown in autoclaved soil (Sunshine professional mix, Sungro) under 12h light (~100 µmol.m^{-2}.s^{-1}) / 12h dark cycles (LD) for 23-25 days at 22°C.

To prepare the infiltration inoculum for the BiFC assay, Agrobacterium GV3101 cells carrying BiFC **pSITE-cEYFP-N1-TOC1, pSITE-EYFP-N1-SII, pSITE-nEYFP-N1-AvrPto and pSITE-nEYFP-N1-SII** or pCB-P19HA vectors were grown over-night in liquid cultures (Luria-Bertani) at 28ºC (shaking at 175rpm) until OD600 between 0.6 and 0.7 was reached (several dilutions were started to assure that a suitable culture was available at the time of treatment). Bacteria were harvested by centrifugation at 3220 x *g* for 2 min, resuspended in 100 mM MgCl2 , harvested by centrifugation at 3220 x *g* for 3 min and finally resuspended in 100 mM MgCl2 adjusting OD600 to 0.5. Cell suspensions carrying pCB-P19HA, **pSITE-nEYFP-N1 and pSITE-cEYFP-N1** vectors were mixed on a 1:1:2 ratio and MG132 (Peptides International) was added to a final concentration of 50 µM. The inoculum was infiltrated into 23-25 day old *N.*

benthamiana leaves, 5 h after lights turned on, using a 1 ml syringe. A 3 mm disc was obtained

from the infiltrated leaves 46 h post infiltration (3 hours after lights turned off) and imaged in the

brighfield and fluorescence channels using a confocal microscope (Zeizz LSM 880) Images were

pseudocolored and overlapped using Fiji (Schindelin et al., 2012).

Yeast two-hybrid assays

To build bait vectors: **pAS-MCS (control), pAS-effectors, pAS-ZTL and pAS-ZTL(LOV), and prey vectors: pACT-MCS (control), pACT-TOC1, pACT-TOC1(PS), pACT-TOC1(IR) and pACT-TOC1(CCT),** protein coding sequences were transferred from

pENTR/D into the pAS-GW (bait) and pACT-GW (prey) vectors (Nakayama et al., 2002) using

LR Clonase II (Life Technologies).

Bait and prey vectors were transformed into the Y187 and AH109 yeast strains,

respectively, as previously described (Walhout et al., 2002). Pairwise combinations of haploid

cells carrying preys and baits were spoted in YPD plates and incubated for 2 days at 28°C. To

select diploid cells carrying preys and baits, cells in each spot were transferred into plates

containing synthetic medium without tryptophane And leucine (SD-WL). Protein-protein

interactions were analyzed based on the expression of *HIS3* and *lacZ* reporter genes. To evaluate

HIS3 expression, diploid cells were plated in SD medium without tryptophan, leucine and

histidine (SD-WLH) supplemented with the HIS3 inhibitor, 3-amino-1,2,4-triazole (3AT) as

indicated in each experiment. Cell growth was determined after 2-3 day incubation at 28°C. To

evaluate *lacZ* expression, β-galactosidase activity was determined in liquid cultures as described

before (Breton et al., 2016).

Yeast three-hybrid assays

To build pBridge-TOC1 bait vector, TOC1 protein coding sequence was PCR amplified from pENTR/D-TOC1 using primers 5'-ATCGCCGGAATTCCCGATGGATTTGAACGGTGAGTG-3' and 5'-GGTCGACGGATCCCCTCAAGTTCCCAAAGCATCATC-3'. The resulting PCR product was cloned into *Sma*I digested pBridge using NEBuilder HiFi DNA Assembly (New England Biolabs).

To build pBridge-TOC1(MET25::AvrPto) and pBridge-TOC1(MET25::AvrPto(Y89D)), AvrPto and AvrPto(Y89D) protein coding sequences were PCR amplified from pENTR/D-AvrPto and pENTR/D-AvrPto(Y89D), respectively, using primers 5'-CCGCATTAGCCCGAAGAATGGGAAATATATGTGTCGG-3' and 5'-GGAGATCAGCCCGAATCATTGCCAGTTACGGTACG-3'. The resulting PCR products were cloned into *Bgl*II digested pBridge-TOC1 using NEBuilder HiFi DNA Assembly (New England Biolabs). Prey constructs pACT-MCS and pACT-ZTL were the same used in yeast two-hybrid experiments.

Bait and prey vectors were transformed into the Y187 and AH109 yeast strains, respectively, as previously described (Walhout et al., 2002). Pairwise combinations of haploid cells carrying preys and baits were spoted in YPD plates and incubated for 2 days at 28°C. To select diploid cells carrying preys and baits, cells in each spot were transferred into plates containing synthetic medium without tryptophane, leucine and methionine (SD-WLmet). Protein-protein interactions were analyzed based on the expression of *HIS3* and *lacZ* reporter genes in the presence or absence of methionine. To evaluate *HIS3* expression, diploid cells were plated in SD medium without tryptophan, leucine and histidine (with or without methionine)

(SD-WLH or SD-WLHmet) supplemented with 3AT (10 mM). Cell growth was determined after 2-3 day incubation at 28°C. To evaluate *lacZ* expression, β-galactosidase activity was determined in SD-WL or SD-WLmet liquid cultures as described before (Breton et al., 2016).

Table S1. Primers used to generate pENTR clones

Effector	Forward primer	Reverse primer
avrE	caccGTGCAGTCACCATCGATC	TTAGCTCTTCAGTTCGAAC
avrPto	caccATGGGAAATATATGTGTC	TCATTGCCAGTTACGGTAC
hopAB2 (avrPtoB)	caccATGGCGGGTATCAATAGAG	TCAGGGGACTATTCTAAAAG
hopA1	caccATGAACCCCATTCAGTCAC	TCATTTCGTGTTTCGAAG
hopB1	caccATGAGACCCGTCGGTGGAC	TCAGACCTTATAGGAAAG
hopC1	caccATGACAATCGTGTCTGGAC	TCAGTGTATTTTTGAAGC
hopD1	caccATGAATCCTCTACGATCTATTC	TCAGGGTGCGGGCTGCCG
hopE1	caccATGAATAGAGTTTCCGGTAG	TCAGTCAATCACATGCGC
hopF2	caccATGGTAATATTTGCGGC	TCAGACCCTTTCGACCGG
hopG1	caccATGCAAATAAAGAACAGTC	TTAGCCGTTGTAAAACTG
hopH1	caccATGATCACTCCGTCTCGATATC	CTATTGATGTGCCCTGTAC
hopI1	caccATGATCAACCTCACCCACATTG	TCATGCCCTATTACCAGC
hopk1	caccATGAATCGCATTTCAACC	TCAGCAGTAGAGCGTGTC
hopM1	caccATGATCAGTTCGCGGATC	TTAACGCGGGTCAAGCAAG
hopN1	caccATGTATATCCAGCAATCTG	TTATCGCAAGTGAAAGTC
hopO1-1	caccATGGGTAATATTTGTGGTAC	TCACTCGTCAGAGCTCTC
hopO1-2	caccATGAATATCAGTCCTGTATC	TCACTCGTCTGAATTATC
hopQ1-1	caccATGCATCGTCCTATCACC	TCAATCTGGGGCTACCGTC
hopR1	caccATGGTCAAGGTTACCTCTTC	CTACACGTTATCGAGTTC
hopS1	caccATGAAAATATCCGGCTCC	TCAGACCTTCCCAAGCTC
hopS2	caccGTGAAAAAGTCTGGCGCTG	TCAGCCAGATGAGCTCGC
hopT1-1	caccATGAAAACAGTCAGCAATC	TCATGACTTTTGAGCCGC
hopT1-2	caccATGATCAAAACAGTCAGC	TCAGCCTACCCGATCAGCG
hopU1	caccATGAATATAAATCGACAAC	TCAAATCTGACTTAATAC
hopV1	caccATGCGGTTTGATGCTGCC	TTACTTTCTATCCGGAATAAC
hopX1	caccATGAAAATACATAACGCTG	TCAGACATCTCGTCTCGC
hopY1	caccATGAACATTACGCCGCTC	TCACTGGTAGTTGATG
hopAA1-1	caccATGCACATCAACCGACGC	TTACGACCGCATAGGCCG
hopAA1-2	caccATGCACATCAACCAATCC	TTACAAACGCCTGAGCTG
hopAF1	caccATGGGGCTATGTATTTCAAAAC	TTATTGTGCGACCAGATG
hopAH1	caccATGAGTATGAATACCTCTG	TCAGGAGAATTGATCCCC
hopAH2-1	caccATGAATATCAATTCAATC	TCAGTATTGATCTGACTT
hopAH2-2	caccATGAACATCCACACCGCC	TCATGAGTACTGATCTGAC
hopAI1	caccATGCTCGCTTTGAAGCTG	TCAGCGAGTCCAGGGCGG
hopAM1-1	caccATGCACGCAAATCCTTTAAG	TTAGTCGCCTAGGAAATTATTTAG
hopAM1-2	caccATGCACGCAAATCCTTTAAG	TTAGTCGCCTAGGAAATTATTTAG
hopAO1	caccATGAATCCCCTGCAACCTATTC	TCATTCTAACGCTATTTTTG

Coding sequence	Forward primer	Reverse primer
TOC1 (stop)	caccATGGATTTGAACGGTGAGTG	TCAAGTTCCCAAAGCATCATC
TOC1 (no stop)	caccATGGATTTGAACGGTGAGTG	AGTTCCCAAAGCATCATCAT
TOC1-PS (stop)	caccATGGATTTGAACGGTGAGTG	TCAGCGTCTTCTTCTCCACATG
TOC1-IR (stop)	caccATGCTAGGACTTGCTGAGAAG	TCAAAGTTTATTTACCCTCACCTC
TOC1-IR (no stop)	caccATGCTAGGACTTGCTGAGAAG	AAGTTTATTTACCCTCACCTC
TOC1-CCT (stop)	caccATGGACAGAAGAGAGGAAGCTCT	TCAAGTTCCCAAAGCATCATC
ZTL (stop)	caccATGGAGTGGG ACAGTGGTTC	TAGCGAGCTA TCTCACGTAA
ZTL-LOV (stop)	caccATGGAGTGGGACAGTGGTTC	TTATGAAGATCCAAGAACAGGTC
ZTL-KELCH (stop)	caccTGGCGAAGGGTTTGTCAGAATG	TTACGTGAGATAGCTCGCTAG
ZTL-FBOX (stop)	caccACAAAAGAAAAGTCAATTGATG	TTAAAGATCCTCATTCTTTGTCAG
MCS	caccATGAGGGAACAAAAGCTGGAGCT	TAGGGCGAATTGGGTACCGGG

References

Agostinelli, C. and Lund, U. (2011). R package circular: Circular Statistics (version 0.4-3). CA Dep. Environ. Sci. Informatics Stat. Ca'Foscari Univ. Venice, Italy. UL Dep. Stat. Calif. Polytech. State Univ. San Luis Obispo, California, USA.

Alabadí, D., Oyama, T., Yanovsky, M.J., Harmon, F.G., Más, P., and Kay, S.A. (2001). Reciprocal regulation between TOC1 and LHY/CCA1 within the Arabidopsis circadian clock. Science (80-.). **293**: 880–883.

Atamian, H.S., Creux, N.M., Brown, E.A., Garner, A.G., Blackman, B.K., and Harmer, S.L. (2016). Circadian regulation of sunflower heliotropism, floral orientation, and pollinator visits. Science (80-.). **353**: 587–590.

Boller, T. and Felix, G. (2009). A Renaissance of Elicitors: Perception of Microbe-Associated Molecular Patterns and Danger Signals by Pattern-Recognition Receptors. Annu. Rev. Plant Biol. **60**: 379–406.

Breton, G., Kay, S.A., and Pruneda-Paz, J.L. (2016). Identification of arabidopsis transcriptional regulators by yeast one-hybrid screens using a transcription factor orfeome. Methods Mol. Biol. **1398**: 107–118.

Chapman, E.J., Prokhnevsky, A.I., Gopinath, K., Dolja, V. V., and Carrington, J.C. (2004). Viral RNA silencing suppressors inhibit the microRNA pathway at an intermediate step. Genes Dev. **18**: 1179–1186.

Curtis, M.D. (2003). A Gateway Cloning Vector Set for High-Throughput Functional Analysis of Genes in Planta. PLANT Physiol. **133**: 462–469.

Djamei, A., Schipper, K., Rabe, F., Ghosh, A., Vincon, V., Kahnt, J., Osorio, S., Tohge, T., Fernie, A., Feussner, I., Feussner, K., Meinicke, P., Stierhof, Y., Schwarz, H., MacEk, B., Mann, M., and Kahmann, R. (2011). Metabolic priming by a secreted fungal effector. Nature **478**: 395–398.

Dodd, A.N. (2005). Plant Circadian Clocks Increase Photosynthesis, Growth, Survival, and Competitive Advantage. Science (80-.). **309**: 630–633.

Gagne, J.M., Downes, B.P., Shiu, S.-H., Durski, A.M., and Vierstra, R.D. (2002). The F-box subunit of the SCF E3 complex is encoded by a diverse superfamily of genes in Arabidopsis. Proc. Natl. Acad. Sci. **99**: 11519–11524.

Godio, R.P. and Martín, J.F. (2009). Modified oxidosqualene cyclases in the formation of bioactive secondary metabolites: Biosynthesis of the antitumor clavaric acid. Fungal Genet. Biol. **46**: 232–242.

Huang, H., Alvarez, S., Bindbeutel, R., Shen, Z., Naldrett, M.J., Evans, B.S., Briggs, S.P., Hicks, L.M., Kay, S.A., and Nusinow, D.A. (2016). Identification of Evening Complex Associated Proteins in Arabidopsis by Affinity Purification and Mass Spectrometry . Mol. Cell. Proteomics **15**: 201–217.

Jones, J.D.G. and Dangl, J.L. (2006). The plant immune system. Nature **444**: 323–329.

Julio, S., Jose, S.-S.J., Southern, M.M., Brown, P.E., and Hall, A. (2006). Luciferases as Reporter Genes. In Arabidopsis Protocols, pp. 293–306.

Li, Z., Bonaldi, K., Uribe, F., and Pruneda-Paz, J.L. (2018). A Localized Pseudomonas syringae Infection Triggers Systemic Clock Responses in Arabidopsis. Curr. Biol.

Lu, S.X., Knowles, S.M., Andronis, C., Ong, M.S., and Tobin, E.M. (2009). CIRCADIAN CLOCK ASSOCIATED1 and LATE ELONGATED HYPOCOTYL Function Synergistically in the Circadian Clock of Arabidopsis. PLANT Physiol. **150**: 834–843.

Makino, S., Kiba, T., Imamura, A., Hanaki, N., Nakamura, A., Suzuki, T., Taniguchi, M., Ueguchi, C., Sugiyama, T., and Mizuno, T. (2000). Genes encoding pseudo-response regulators: Insight into His-to-Asp phosphorelay and circadian rhythm in Arabidopsis thaliana. Plant Cell Physiol. **41**: 791–803.

Marshall, C.M., Tartaglio, V., Duarte, M., and Harmon, F.G. (2016). The Arabidopsis sickle Mutant Exhibits Altered Circadian Clock Responses to Cool Temperatures and Temperature-Dependent Alternative Splicing . Plant Cell **28**: 2560–2575.

Más, P., Alabadí, D., Yanovsky, M.J., Oyama, T., and Kay, S.A. (2003a). Dual role of TOC1 in the control of circadian and photomorphogenic responses in Arabidopsis. Plant Cell **15**: 223–36.

Más, P., Kim, W.Y., Somers, D.E., and Kay, S.A. (2003b). Targeted degradation of TOC1 by ZTL modulates circadian function in Arabidopsis thaliana. Nature **426**: 567–570.

Mathieu, J., Schwizer, S., and Martin, G.B. (2014). Pto Kinase Binds Two Domains of AvrPtoB and Its Proximity to the Effector E3 Ligase Determines if It Evades Degradation and Activates Plant Immunity. PLoS Pathog. **10**.

McClung, C.R. (2006). Plant Circadian Rhythms. PLANT CELL ONLINE **18**: 792–803.

Michael, T.P., Salomé, P.A., Yu, H.J., Spencer, T.R., Sharp, E.L., McPeek, M.A., Alonso, J.M., Ecker, J.R., and McClung, C.R. (2003). Enhanced Fitness Conferred by Naturally Occurring Variation in the Circadian Clock. Science (80-.). **302**: 1049–1053.

Nakamichi, N., Kiba, T., Henriques, R., Mizuno, T., Chua, N.H., and Sakakibara, H. (2010). PSEUDO-RESPONSE REGULATORS 9, 7, and 5 Are Transcriptional Repressors in the Arabidopsis Circadian Clock. Plant Cell **22**: 594–605.

Nakayama, M., Kikuno, R., and Ohara, O. (2002). Protein-protein interactions between large proteins: Two-hybrid screening using a functionally classified library composed of long cDNAs. Genome Res. **12**: 1773–1784.

Nürnberger, T. and Brunner, F. (2002). Innate immunity in plants and animals: Emerging parallels between the recognition of general elicitors and pathogen-associated molecular patterns. Curr. Opin. Plant Biol. **5**: 318–324.

Pitzschke, A. and Hirt, H. (2009). Disentangling the Complexity of Mitogen-Activated Protein Kinases and Reactive Oxygen Species Signaling. PLANT Physiol. **149**: 606–615.

Plautz, J.D., Straume, M., Stanewsky, R., Jamison, C.F., Brandes, C., Dowse, H.B., Hall, J.C., and Kay, S.A. (1997). Quantitative Analysis of Drosophila period Gene Transcription in Living Animals. J. Biol. Rhythms **12**: 204–217.

Putterill, J. (2001). Flowering in time: Genes controlling photoperiodic flowering in Arabidopsis. In Philosophical Transactions of the Royal Society B: Biological Sciences, pp. 1761–1767.

Rijo-Ferreira, F., Carvalho, T., Afonso, C., Sanches-Vaz, M., Costa, R.M., Figueiredo, L.M., and Takahashi, J.S. (2018). Sleeping sickness is a circadian disorder. Nat. Commun. **9**.

Schindelin, J. Arganda-Carreras, I., and Frise, E. (2012). Fiji: an open-source platform for biological-image analysis. Nat. Methods **9**: 676–82.

Schmittgen, T.D. and Livak, K.J. (2008). Analyzing real-time PCR data by the comparative C(T) method. Nat. Protoc. **3**: 1101–8.

Somers, D.E., Webb, A.A., Pearson, M., and Kay, S.A. (1998). The short-period mutant, toc1-1, alters circadian clock regulation of multiple outputs throughout development in Arabidopsis thaliana. Development **125**: 485–94.

Strayer, C., Oyama, T., Schultz, T.F., Raman, R., Somers, D.E., Mas, P., Panda, S., Kreps, J.A., and Kay, S.A. (2000). Cloning of the Arabidopsis clock gene TOC1, an autoregulatory response regulator homolog. Science (80-.). **289**: 768–771.

Sundar, I.K., Ahmad, T., Yao, H., Hwang, J.W., Gerloff, J., Lawrence, B.P., Sellix, M.T., and Rahman, I. (2015). Influenza A virus-dependent remodeling of pulmonary clock function in a mouse model of COPD. Sci. Rep. **4**.

Walhout, A.J.M., Boulton, S.J., and Vidal, M. (2002). Yeast Two-Hybrid Systems and Protein Interaction Mapping Projects for Yeast and Worm. Yeast **1**: 88–94.

Wei, W., Plovanich-Jones, A., Deng, W.-L., Jin, Q.-L., Collmer, A., Huang, H.-C., and He, S.Y. (2000). The gene coding for the Hrp pilus structural protein is required for type III secretion of Hrp and Avr proteins in Pseudomonas syringae pv. tomato. Proc. Natl. Acad. Sci. **97**: 2247–2252.

Wenkel, S., Turck, F., Singer, K., Gissot, L., Le Gourrierec, J., Samach, A., and Coupland, G. (2006). CONSTANS and the CCAAT Box Binding Complex Share a Functionally Important Domain and Interact to Regulate Flowering of Arabidopsis. PLANT CELL ONLINE **18**: 2971–2984.

Zhang, C., Xie, Q., Anderson, R.G., Ng, G., Seitz, N.C., Peterson, T., McClung, C.R., McDowell, J.M., Kong, D., Kwak, J.M., and Lu, H. (2013). Crosstalk between the Circadian Clock and Innate Immunity in Arabidopsis. PLoS Pathog. **9**.

Zhang, X., Henriques, R., Lin, S.S., Niu, Q.W., and Chua, N.H. (2006). Agrobacterium-mediated transformation of Arabidopsis thaliana using the floral dip method. Nat. Protoc. **1**: 641–646.